JOURNAL OF CATALYSIS **141**, 465–477 (1993)

Infrared Spectroscopy of Adsorbed Carbon Monoxide on Platinum/Nonacidic Zeolite Catalysts

G. S. LANE,[1] J. T. MILLER, F. S. MODICA, AND M. K. BARR

Amoco Oil Company, P.O. Box 3011, Naperville, Illinois 60566

Received April 29, 1992; revised December 22, 1992

Infrared spectroscopy of adsorbed carbon monoxide was investigated on a series of platinum (or palladium) zeolite catalysts plus platinum on silica. The platinum catalysts all showed a strong absorbance band around 2070 ± 20 cm^{-1} due to linear-bonded CO and a weaker band around 1850 ± 20 cm^{-1} due to bridge-bonded CO. Four platinum catalysts, Pt/K^+ LTL, Pt/K^+ MFI, Pt/K^+ MTW, and Pt/K^+ SiO_2, had an additional absorbance near 1970 cm^{-1}. The additional band is *not* observed for Pt/silica, Pt/La^{+3} LTL, or platinum supported on H^+ LTL or H^+ MFI, i.e., neutral and acidic supports. The additional band on the alkalized catalysts is speculated to result from an electrostatic attraction of linear-bonded CO with an alkali cation when Pt is on a nonacidic support. The electrostatic attraction increases the CO adsorption strength and lowers the stretching frequency. The additional linear CO absorption band was also observed on Pd/K^+ LTL. The additional band, therefore, is not specific to platinum. Although the presence of this additional infrared band suggests a "new type of metal (catalytic) site," no relation was found between the catalytic activity or selectivity for *n*-hexane dehydrocyclization and the additional CO absorbance band. © 1993 Academic Press, Inc.

INTRODUCTION

Infrared spectroscopy of adsorbed species is an established technique for characterizing surface sites in highly dispersed, supported metal catalysts. In particular, CO is frequently used as the adsorbing molecule because of its high extinction coefficient, which gives strong absorbances when adsorbed on Group VIII metals (*1–3*). Most of the prior work on platinum catalysts has focused on amorphous supports, such as platinum on alumina (*3–10*) or silica (*3, 4, 7, 11–14*). In these studies, linear- and bridge-bonded CO species have been assigned to bands absorbing at 2040–2100 cm^{-1} and 1790–1860 cm^{-1}, respectively (*3, 15*). Similar frequencies are reported for unsupported platinum, i.e., single crystals (*3, 16–22*). The location of the CO stretching frequency is known to shift, and several interpretations have been postulated. For example, the shift in stretching frequency may be due to dilution effects (dipole–dipole interactions), changes in the exposed platinum crystallite faces (particle size), or electron density changes induced by the catalyst support or cations, which affects the number of electrons available for back-bonding to the CO π^* orbitals.

Platinum supported on zeolites is particularly interesting since the average metal particle size can be kept uniformly small, with the size of the largest metal particles limited to the size of the zeolite pore(s) or cage(s). A recent review (*23*) suggests that these catalysts combine the intrinsic electronic effects of a small metal particle (*24*) with electronic modifications resulting from the interaction of the metal particle with the strong ionic potential of the zeolite surface (*25–29*). For example, the infrared spectra for palladium supported on acidic and nonacidic FAU(Y) exhibits one linear- and one

---

[1] To whom correspondence should be addressed at Amoco Research Center, P.O. Box 3011, Mail Station H-6, Naperville, IL 60566.

0021-9517/93 $5.00

bridge-bonded CO absorption. In addition, the palladium interacts with the acid sites, shifting the CO stretching frequency to higher wavenumbers. This shift to higher frequency is suggested to result from electron-deficient palladium. By interacting with the acid sites, palladium has fewer metal electrons to π-bond with adsorbed CO (*25*). Generally, platinum in nonacidic zeolites, e.g., Na^+ FAU(Y), also exhibits one linear and one bridging CO infrared frequency (*24*). For platinum supported on nonacidic LTL, however, three CO absorption bands have been reported (*30–32*). In addition to the usual linear- and bridge-bonded stretching frequencies, nonacidic LTL displayed an additional absorbance band centered around 1970 cm^{-1}. The exact position of the CO absorbance was dependent on the specific cation (Li^+, Na^+, K^+, Rb^+, or Cs^+) exchanged into the zeolite. The frequency shifted to lower wavenumbers for the larger, more basic cation, e.g., Cs^+. The additional band was assigned to linearly adsorbed CO located on the very small Pt particles within the zeolite channels, which were thought to form (basic) carbonyl clusters on exposure to CO (*31*). Three infrared CO absorption bands have also been observed for a Pt/Na^+ FAU(X) or FAU(Y) after heating the catalyst to 573 K for 16 h in CO (*33*). This additional band was absent, however, without heating. For platinum in Na^+ FAU(X), the additional absorption band was thought to result from CO linearly adsorbed on electron-rich platinum atoms in contact with negatively charged framework oxygen atoms in aluminum-rich zeolites. The frequency of the additional band decreased with increasing (zeolite) oxide basicity. Comparison of catalytic activity for *n*-hexane dehydrocyclization for Pt/Na^+ FAU(X), Pt/K^+ LTL, and Pt/Na^+ FAU(Y) parallels the catalysts' basicity. It was suggested that the most active platinum atoms for *n*-hexane aromatization were the atoms in contact with the zeolite surface, activated by the negatively charged framework oxygen atoms (*33*).

In this study, we compare the infrared spectra of CO adsorbed on a series of platinum-supported catalysts. The supports include nine potassium-exchanged zeolites, SiO_2, and K^+ SiO_2. The potassium-exchanged zeolites are nonacidic and have the platinum located in the zeolite pores. Several of the catalysts exhibited three CO absorption bands. For these catalysts, platinum in acidic zeolites of the same structure was prepared for comparison. For the nonacidic platinum catalysts, the activity and selectivity for dehydrocyclization of *n*-hexane was determined, and the catalytic performance was compared with the catalysts' infrared spectra. Finally, palladium-supported, nonacidic LTL catalysts showed that the third CO absorption band was not specific to platinum.

EXPERIMENTAL

Catalyst Preparation

Catalysts were prepared from nonacidic, potassium-exchanged supports by impregnating a platinum (or palladium) salt, decomposing the metal salt, and reducing the metal. The zeolites were obtained as commercial samples or were synthesized. Na^+ FAU(Y), Na^+ FAU(X), and K^+ LTL were commercial samples obtained from Union Carbide (now UOP). Na^+ MOR was a commercial sample obtained from Norton.

MFI (ZSM-5) (*34*), ZSM-12 (MTW) (*35*), Na^+ gmelinite (GME) (*36*), Na^+ Ω (MAZ) (*37*), and β (*38*) zeolites were synthesized following reported methods. For zeolites prepared with organic amine, the zeolites were calcined at 540°C for 16 h prior to potassium exchange. Each zeolite (except LTL) was potassium exchanged with KNO_3. Typically, 75 g of zeolite was exchanged with 500 ml 1.5 *M* KNO_3 at 60°C for 4 h. The exchanged zeolite was filtered, washed with 500 ml cold H_2O, and refiltered. The K^+-exchanged zeolite was given a second wash with dilute KOH. The pH of the 500 ml water wash was adjusted to 9.5 with KOH. The zeolite was filtered, dried, and

TABLE 1

Elemental Analysis

Catalyst	Potassium (wt%)	Sodium (wt%)	Aluminum (wt%)	Cation/Al (mole ratio)
K^+ FAU(Y)	10.20	2.73	9.30	1.10
K^+ FAU(X)	11.50	6.67	15.60	1.01
K^+ β	4.100	—	2.58	1.10
K^+ MOR	10.00	0.04	5.90	1.18
K^+ MAZ	11.0	—	7.00	1.08
K^+ GME	11.90	1.15	9.50	1.00
K^+ MTW	1.45	—	0.99	1.01
K^+ MFI	2.28	—	1.35	1.16
K^+ LTL	11.75	—	7.73	1.05
Ba^{2+} LTL	9.70	(7.2 Ba)	8.0	1.19
La^{3+} LTL	6.40	(4.3 La)	7.10	0.98
H^+ LTL	5.60	—	11.50	0.34
H^+ MFI	—	—	2.20	0.00
K^+ SiO_2	0.60	—	—	—

calcined at 540°C for 3 h. Table 1 summarizes a partial elemental analysis of each support.

Other ion-exchanged zeolites were prepared as briefly described below. A Ba^{2+} LTL support was synthesized by ion exchange of K^+ LTL with 0.6 *M* $Ba(NO_3)_2$ at 60°C for 2 h. A H^+ LTL was prepared by ion exchange of 130 g of K^+ LTL in 1000 ml of 1.5 *M* NH_4NO_3 at 60°C for 2 h. The exchanged zeolites were filtered, washed with 500 ml of hot water, dried overnight, and calcined at 540°C for 3 h. To prepare H^+ MFI, following the synthesis of MFI, the zeolite was calcined at 540°C for 16 h to remove the tetrapropylammonium bromide. The zeolite was exchanged three times with 1.5 *M* NH_4NO_3, washed, dried, and calcined at 500°C for 3 h. Finally, La^{3+} LTL was prepared by ion exchange of K^+ LTL with 0.2 *M* $La(NO_3)_3 \cdot 5H_2O$ (40 g/500 ml H_2O). The zeolite was ion exchanged twice, washed, dried, and calcined at 540°C for 3 h.

The SiO_2 catalysts were prepared from silica (PQ Corporation) with a surface area of 215 m^2/g and a pore volume of 1.0 cm^3/g. Alkalized silica was prepared by addition of dilute KOH to the silica. The KOH was continually added until the pH of the solution remained 9.5. The alkalized silica was filtered, dried, and calcined at 540°C for 4 h.

To each zeolite (or silica), platinum was impregnated using an aqueous solution of tetraammineplatinum(II) nitrate to a weight loading of 1.0% platinum. Platinum-impregnated zeolites were calcined in air at 260°C and then reduced in hydrogen at 500°C. In a similar fashion, the palladium catalysts were prepared using an aqueous solution of tetraamminepalladium(II) nitrate to weight loadings of 0.5% palladium.

Infrared Spectroscopy

Sample preparation. Typically, a reduced catalyst sample was ground to a fine, uniform powder. Catalyst wafers were formed by compressing 100 mg in a 1.25-in. (3.18 cm) diameter, gold-plated, stainless-steel die with a pressure of 9.0 metric tons. The wafer of approximately 10 mg/cm^2 was trimmed to 30 × 11 mm and mounted into a quartz sample holder, and the vacuum system was sealed.

Infrared procedure. The vacuum manifold, sample chamber, and infrared cell assembly were evacuated to a pressure less than 10^{-4} Torr. The sample was then rereduced *in situ* by admitting hydrogen to a pressure of 50 Torr, followed by heating to 480°C for 1 h. After reduction, the hydrogen was evacuated to less than 10^{-4} Torr for 15 min at 480°C. The sample was cooled to room temperature and lowered into the infrared beam (Nicolet 740). The entire spectral region was scanned to obtain a reference spectrum of the reduced catalyst. Spectral resolution was 4 cm^{-1} for all spectra.

Following reduction and evacuation, research grade CO (99.999%) was admitted from a glass bulb to a pressure of 8.0 Torr at ambient temperature. A second spectrum was collected. The background (reference) spectrum was digitally subtracted from the CO absorbance spectrum.

RESULTS

For each of the zeolite catalysts, transmission electron microscopy verified that the platinum was within the zeolite pores with no large external platinum particles. At high resolution, the largest platinum particles appeared to fill some of the zeolite pores or cages. Electron micrographs of several catalysts prepared by these methods have been reported elsewhere (*39*, *40*).

Infrared Spectroscopy

Potassium-exchanged zeolites. Nine platinum on potassium-exchanged zeolites were examined by infrared spectroscopy to determine the number and frequency of CO absorption bands. For comparison, the infrared spectra of platinum on SiO_2 was also obtained. The spectra reveal significantly different features among the catalysts. Most of the catalysts, Pt/SiO_2, Pt/K^+ FAU(Y), Pt/K^+ FAU(X), Pt/K^+ MOR, Pt/K^+ GME, Pt/K^+ MAZ, and Pt/K^+ β, exhibit a typical CO absorption spectrum with a band at 2040–2100 cm^{-1} due to linear-bonded CO and a second, broader band located around 1790–1860 cm^{-1} due to bridge-bonded CO. Representative spectra are given in Fig. 1. Generally, the absorption bands on the zeolites are broader than the corresponding bands on amorphous catalysts; for example, compare the infrared spectrum of Pt/SiO_2 with the Pt/zeolite catalysts in Fig. 1. Table 2 summarizes the location for the major bands for each catalyst.

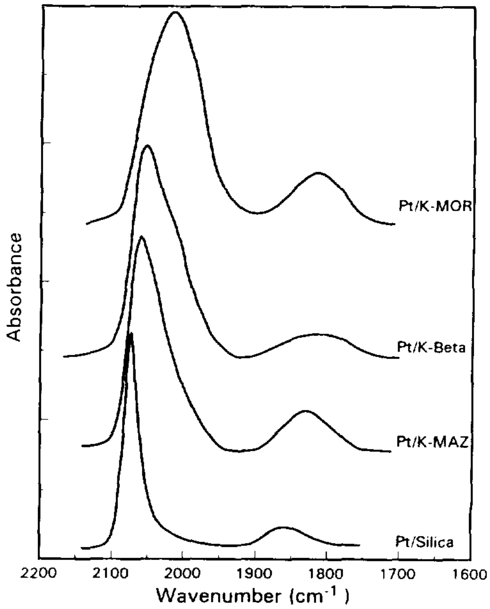

FIG. 1. Infrared spectra of CO adsorbed on Pt/K^+ MOR, Pt/K^+ β, Pt/K^+ MAZ, and Pt/silica at 8.0 Torr CO and room temperature after reduction and evacuation at 480°C.

Unlike the spectra of Fig. 1, the infrared spectrum of CO adsorbed on Pt/K^+ LTL, Fig. 2, displays an additional absorbance around 1960 cm^{-1}. Depending on the method of preparation and the pretreatment procedure, the location of the additional absorbance band was found to shift (less than 10 wavenumbers) and change in intensity relative to the absorbance band assigned to linear-bonded CO, 2060 cm^{-1}. Also shown in Fig. 2 are the spectra for Pt/K^+ MFI and Pt/K^+ MTW. Both of these catalysts display a third CO absorption band, previously observed for Pt/K^+ LTL (*30–32*). The additional infrared absorbance observed for each of these catalysts was developed by exposure to CO at room temperature and did not require heating overnight at 573 K in CO as required for Na^+ FAU(Y)

TABLE 2

Infrared Absorbance of CO Adsorbed on Platinum Catalysts

Catalyst	Linear-bonded CO (2020–2090 cm^{-1})	Additional band (1890–2000 cm^{-1})	Bridge-bonded CO (1775–1850 cm^{-1})
Pt/SiO$_2$	2075	nd	1900
Pt/K$^+$ FAU(Y)	2020	nd	1780
Pt/K$^+$ FAU(X)	2045	nd	1800
Pt/K$^+$ β	2055	nd	1820
Pt/K$^+$ MOR	2050	nd	1820
Pt/K$^+$ MAZ	2070	nd	1840
Pt/K$^+$ GME	2030	nd	1790
Pt/K$^+$ MTW	2050	1890	1810
Pt/K$^+$ MFI	2055	2000	1778
Pt/K$^+$ LTL	2060	1960	1790

Note. nd, not detected.

(*33*). Table 2 also summarizes the locations of the band maxima for these three catalysts. Although we refer to the additional absorbance as a single band, it could be resolved into multiple bands whose positions and relative intensities were a function of catalyst preparation, pretreatment, and CO dosing procedure. For simplicity, we continue to refer to this absorbance band or group of absorbance bands as an additional absorbance.

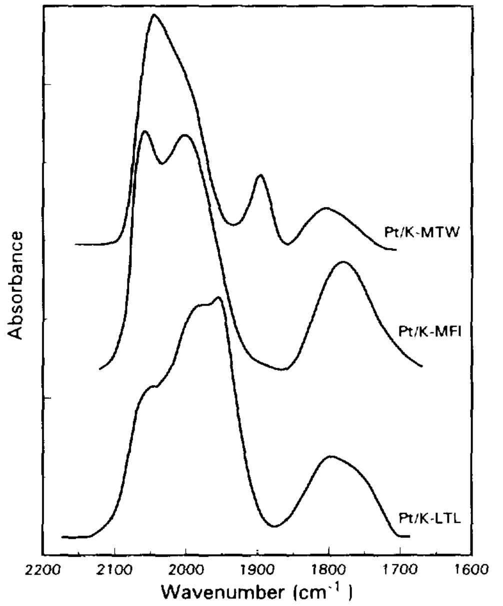

FIG. 2. Infrared spectra of CO adsorbed on Pt/K$^+$ MTW, Pt/K$^+$ MFI, and Pt/K$^+$ LTL at 8.0 Torr CO and room temperature after reduction and evacuation at 480°C.

Following saturation of Pt/K$^+$ LTL with CO, the catalyst was evacuated to partially remove CO. The stretching frequency for both the linear CO absorption, e.g., at 2075 cm^{-1}, and the additional absorption at 1960 cm^{-1}, shifted to lower frequency with decreasing surface coverage. In addition, the intensity of the linear band decreased more rapidly than the intensity of the additional band. The additional band apparently reflects CO chemisorbed more strongly than linearly adsorbed CO. Since the band intensities decrease independently, it is unlikely that the two bands result from a symmetric and antisymmetric stretch from a *gem*-dicarbonyl as observed for supported rhodium (*41*). Adsorption of CO at pressures from 0.0003 to 8.3 Torr, i.e., increasing surface coverage, indicates that the linear band and additional band develop before the bridging CO band. In addition, the intensity of the new band develops at lower pressure compared with the linear band. Adsorption and desorption of CO indicate that the additional band is independent of the linear band, but behaves similar to the linear band.

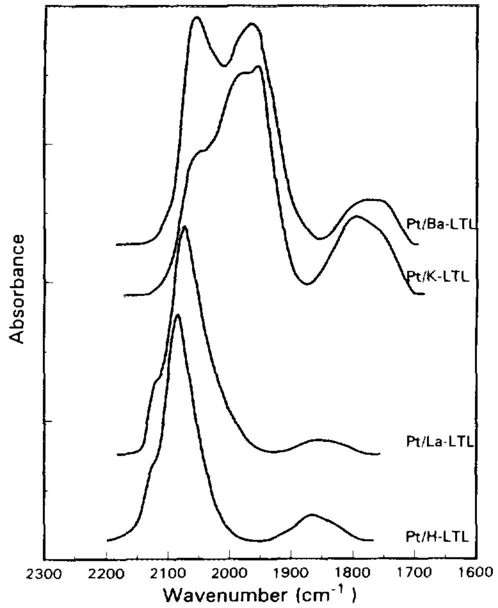

FIG. 3. A comparison of infrared spectra of CO adsorbed on various ion-exchanged LTL catalysts at 8.0 Torr CO and room temperature after reduction and evacuation at 480°C.

The effect of support acidity. Figures 3 and 4 show the CO absorption spectra for platinum supported on potassium and hydrogen forms of LTL and MFI, respectively. For both catalysts, three CO absorption bands are observed on the nonacidic, potassium-exchanged zeolite, but only two CO bands are present on the acidic, H-zeolites. For Pt/H$^+$ LTL and Pt/H$^+$ MFI, both the linear- and bridge-bonded CO are shifted to higher frequency compared with the potassium-exchanged zeolite. The locations of the band maxima are given in Table 3. Similarly, addition of alkali to Pt/SiO$_2$ also affects its infrared spectrum (Fig. 5). For Pt/SiO$_2$, two CO absorbances are observed, while for Pt/K$^+$ SiO$_2$, three CO absorbances are observed. As observed for H$^+$ LTL and H$^+$ MFI, the linear- and bridge-bonded bands are shifted to higher frequency in the alkali-free SiO$_2$ catalyst, e.g., Pt/SiO$_2$. While H$^+$ LTL and H$^+$ MFI have strong Brønsted acidity, SiO$_2$ does not. The appearance of the additional infrared band, therefore, requires the presence of alkali or basic supports. Although this seems to be necessary, it is not a sufficient condition for development of the additional band. For example, catalysts in Fig. 1 contain alkali and are nonacidic, yet display only two infrared bands, i.e., one linear- and one bridge-bonded CO absorption band.

Although different alkali cations cause the CO infrared bands to shift, the additional band is only observed on nonacidic LTL, MTW, MFI, or SiO$_2$. In a previous study of Pt/LTL, the location of each infrared band shifted to lower frequency as the alkali cation was changed from Li$^+$, Na$^+$, K$^+$, Rb$^+$, to Cs$^+$ (*31*). For each alkali-exchanged Pt/LTL catalyst, however, the new band located near 1970 cm^{-1} was present. Figure 3 shows that the three absorption bands are also present on Pt/Ba^{2+} LTL. The locations of the absorption frequencies have been summarized in Table 3. Although three infrared CO absorption bands are present in Pt/K$^+$ LTL and Pt/Ba^{2+} LTL, when LTL

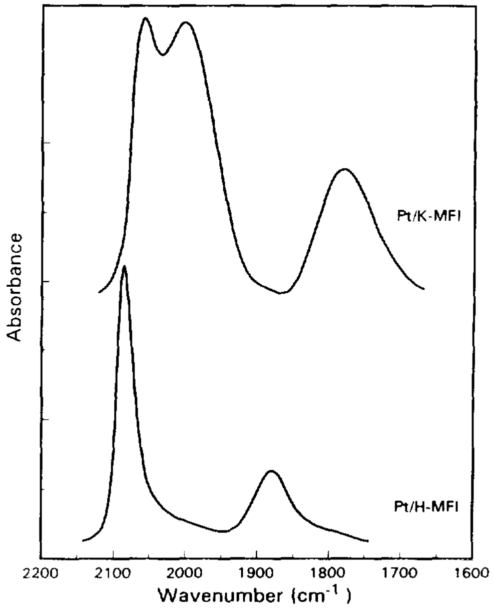

FIG. 4. A comparison of infrared spectra of CO adsorbed on K$^+$- and H$^+$-exchanged MFI catalysts at 8.0 Torr CO and room temperature after reduction and evacuation at 480°C.

TABLE 3

Infrared Absorbance of CO on Acidic and Nonacidic Platinum Catalysts

Catalyst	Linear-bonded CO (2020–2090 cm^{-1})	Additional band (1890–2000 cm^{-1})	Bridge-bonded CO (1775–1850 cm^{-1})
Pt/K^+ LTL	2060	1960	1790
Pt/Ba^{2+} LTL	2060	1965	1750
Pt/H^+ LTL	2090	nd	1875
Pt/La^{3+} LTL	2075	nd	1850
Pt/K^+ MFI	2055	2000	1778
Pt/H^+ MFI	2085	nd	1877
Pt/K^+ SiO_2	2050	1990	1775
Pt/SiO_2	2075	nd	1900

Note. nd, not detected.

is lanthanum exchanged, the band at 1970 cm^{-1} is absent. Figure 3 shows the infrared spectrum for Pt/La^{3+} LTL with the absorption frequencies given in Table 3. Similar to what was observed for Pt/H^+ LTL, the two CO absorption bands on Pt/La^{3+} LTL have shifted to higher frequency compared with Pt/K^+ LTL.

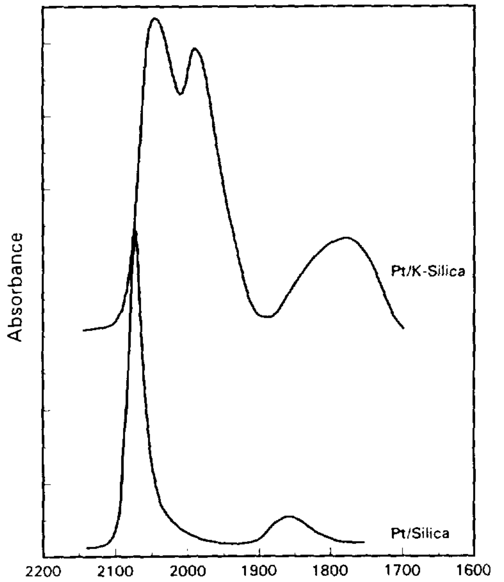

FIG. 5. Infrared spectra of CO adsorbed on Pt/K^+ silica and Pt/silica at 8.0 Torr CO and room temperature after reduction and evacuation at 480°C.

Palladium. The infrared spectra of CO adsorbed on four palladium/zeolite catalysts were also obtained. The catalysts were palladium on K^+ FAU(Y), Na^+ FAU(Y), K^+ LTL, and Ba^{2+} LTL. The FAU(Y) catalysts exhibited the infrared spectra that have been observed for palladium catalysts, that is, a linear-bonded CO band around 2070 cm^{-1} and a strong bridge-bonded band around 1820 cm^{-1} (*25, 26*). Since these spectra are similar to those previously reported, the spectra are not shown; however, the band positions are given in Table 4. In contrast to FAU, infrared spectra of both Pd/K^+ LTL and Pd/Ba^{2+} LTL exhibit three CO absorption bands, with an additional absorption located around 1970 cm^{-1}. The frequency of the additional band on Pd/K^+ LTL is similar to that on Pt/K^+ LTL. The size and shape of the additional infrared absorbance at 1970 cm^{-1} for Pd/K^+ LTL is much smaller and sharper than the bridging band at 1850 cm^{-1}. The additional band is similar in intensity and half-width to the linear-bonded CO band at 2075 cm^{-1}. Figure 6 shows the infrared spectra for CO adsorbed on the Pd/K^+ LTL and Pd/Ba^{2+} LTL. The frequencies of the infrared bands are given in Table 4.

Catalytic results. The platinum, nonacidic catalysts were tested at 400°C in an atmospheric, continuous-flow, fixed-bed reactor for conversion of *n*-hexane to ben-

TABLE 4

Infrared Absorbance of CO Adsorbed to Palladium Catalysts

Catalyst	Linear-bonded CO (2020–2090 cm^{-1})	Additional band (1890–2000 cm^{-1})	Bridge-bonded CO (1775–1850 cm^{-1})
Pd/K$^+$ FAU(Y)	2070	nd	1820
Pd/Na$^+$ FAU(Y)	2075	nd	1850
Pd/K$^+$ LTL	2075	1965	1850
Pd/Ba^{2+} LTL	2075	1975	1840

Note. nd, not detected.

zene. The experimental apparatus and procedure have been described previously (*40*). Throughout a catalyst test (approximately 6 h), the nonacidic catalysts displayed no change in activity or selectivity. In addition to benzene, the reaction products included light (C_1–C_5) gases, methylcyclopentane, 2-methylpentane, and 3-methylpentane. Methylcyclopentane, 2-methylpentane, and 3-methylpentane result from one-five ring closure of *n*-hexane, while benzene results from one-six ring closure (*40, 42*). The selectivity to reaction products, at 10% conversion, is given in Table 5 along with the ratio for ring closure reactions, e.g., the ratio of one-six to one-five ring closure. For each catalyst, except Pt/K$^+$ LTL and Pt/K$^+$ MAZ, the ratio of one-five/one-six ring closure is nearly constant at 0.5. Not only do these catalysts favor one-five ring closure, but the (ring closure) selectivity differences among the catalysts are small. For Pt/K$^+$ MAZ, however, there is an increase in the selectivity for one-six ring closure, i.e., higher benzene selectivity, although the rate of one-five ring closure is still higher than one-six ring closure. In Pt/K$^+$ LTL, the benzene selectivity is further increased, and the rate of one-six ring closure exceeds the one-five ring closure rate.

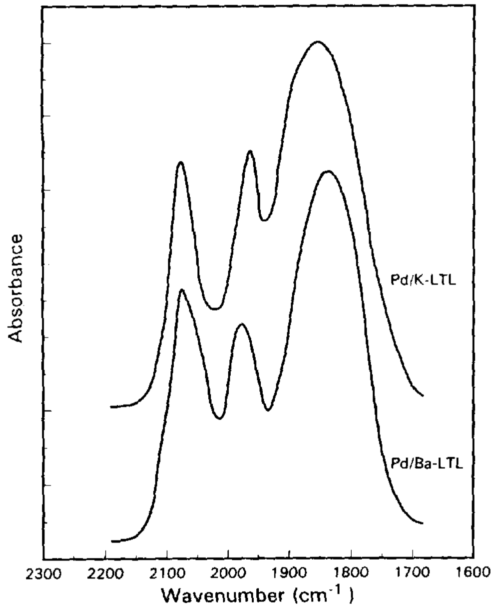

FIG. 6. Infrared spectra of CO adsorbed on Pd/K$^+$ LTL and Pd/Ba^{2+} LTL at 8.0 Torr CO and room temperature after reduction and evacuation at 480°C.

Catalyst activities are given in Table 6 and were calculated in two ways. First, the relative activity per gram of catalyst was determined by the weight of catalyst required to affect constant conversion. The Pt/K$^+$ SiO_2 was assigned a relative activity of 1.0. Since the CO chemisorption capacity in each catalyst is different, the specific activity, i.e., the activity per exposed platinum, for the rate of formation of benzene is also given in Table 6. The platinum surface areas were determined by H_2 chemisorption. Despite the differences in pore and cavity sizes, all the zeolite catalysts were more active than the Pt/K$^+$ SiO_2. Among the potassium-exchanged zeolites, Pt/K$^+$ LTL and Pt/K$^+$ MAZ were highly active, with Pt/K$^+$ β the most active for conversion

TABLE 5

n-Hexane Reaction Productions

Catalyst	Product selectivities[a]			
	C_1–C_5	One-five	One-six	One-five
		Ring closure[b]	Ring closure (benzene)	
MFI	0.20	0.52	0.28	0.54
MTW	0.15	0.56	0.29	0.52
GME	0.20	0.53	0.27	0.51
β	0.14	0.56	0.30	0.53
MAZ	0.11	0.48	0.41	0.85
LTL	0.09	0.41	0.50	1.25
FAU(Y)	0.06	0.67	0.27	0.40
FAU(X)	0.11	0.69	0.20	0.29
K^+ SiO_2	0.12	0.59	0.29	0.49

[a] Selectivities determined at 10% conversion.

[b] One-five ring closure is defined as the sum of methylcyclopentane, 2-methylpentane, and 3-methylpentane (*40*).

of *n*-hexane. These catalysts were also the most active for formation of benzene.

DISCUSSION

Previously, three CO infrared absorption bands for platinum/zeolite catalysts have been reported for alkali-exchange LTL (*30–32*) and for Na^+ FAU(X) after heating overnight at 573 K in CO (*33*) It was suggested that the additional infrared band in Pt/K^+ LTL resulted from CO linearly adsorbed on very small, internal platinum particles, while the band at 2060 cm^{-1} was thought to result from CO adsorbed on larger, internal particles of approximately 1.0 to 2.5 nm (*30*). Figures 2, 5, and 6 show that the band near 1970 cm^{-1} is not unique to nonacidic LTL, nor specific to platinum. From TEM, each of the catalysts was determined to have all of the platinum (or palladium) located within the zeolite pores. In Pt/K^+ LTL, for example, there are few particles larger than 1.0 nm visible by TEM (*40*). In addition, EXAFS confirms that the average particle size is very small (*43*). Nevertheless, three CO infrared absorbance bands are observed for Pt/K^+ LTL with small particles. With the absence of large internal particles, the linear absorbance band cannot be attributed to large internal platinum particles. Therefore, the linear band and the additional band in the infrared spectra of Pt/K^+ LTL, Pt/K^+/MFI, Pt/K^+ MTW, and Pt/K^+ SiO_2 must be associated with the small metal particles located within the zeolite pores.

TABLE 6

Catalyst Activities

Catalyst	*n*-Hexane[a]	Benzene[a]	Benzene TOF[b]
K^+ SiO_2	1.0	1.0	0.0066
K^+ MFI	4.0	3.6	0.38
K^+ MTW	5.4	5.2	0.38
K^+ GME	5.8	5.4	0.11
K^+ β	16.6	17.2	0.21
K^+ MAZ	7.3	10.3	0.12
K^+ LTL	10.0	17.2	0.37
K^+ FAU(Y)	5.0	5.2	0.076
K^+ FAU(X)	4.5	3.1	0.057

[a] K^+ SiO_2 is defined as 1.0 Relative Activity.

[b] (Absolute) Turnover frequency (TOF), based on H_2 Chemisorption, at 400°C and 1 atm.

In previous studies of metal catalysts displaying three infrared CO absorbances, there has been little agreement on the origin of the additional band near 1970 cm^{-1} (*9, 10, 13, 14, 30–33*). For Pt/Al_2O_3 (*9*), the additional band was attributed to CO linearly bonded on high Miller index Pt atoms, i.e., the step and corner Pt atoms. The number of these atoms should directionally increase in catalysts with small platinum particles. This explanation, however, is not consistent with the presence of the third band on potassium LTL, MFI, and MTW and the absence of the band in the H^+ zeolites. It likewise does not explain why the third infrared band is absent in the other potassium-exchanged zeolites, for example, Fig. 1. In all the zeolite catalysts, the Pt particles are extremely small, and one would not necessarily expect to have smaller particles, with an increase in the number of steps and corners, only for K^+ LTL, K^+ MFI, and K^+ MTW. In fact, recent EXAFS analyses indicate that the platinum particles are slightly smaller on Pt/H^+ LTL than on Pt/K^+ LTL (*44*).

Two other possible hypotheses have also been proposed. The first proposal suggests that the additional band results from CO adsorbed on platinum with increased electron density. The increased electron density results from the interaction of platinum with the strongly negative oxide-surface ions (*30, 31, 33*). According to this hypothesis, in aluminum-rich zeolites, e.g., FAU(X) and LTL, the oxide ions of the support are strongly basic with a large, local negative charge. The strongly negative-oxide ions, which are adjacent to platinum atoms, are thought to interact, donating electron density to those platinum atoms. The increased electron density of the platinum results in increased bonding to the CO π^* orbitals decreasing the infrared stretching frequency (*33*). Since three CO absorption bands are observed for Pt/K^+ MFI and Pt/K^+ MTW, which contain 1.35 and 0.99 wt% Al, respectively, it does not appear that aluminum-rich zeolites are the only catalysts that may show the new infrared absorbance. Indeed, three infrared bands are observed on Pt/K^+ SiO_2, Fig. 5, and in Ref. (*14*), and this catalyst does not contain aluminum. Although the aluminum content of the zeolite does not appear to directly determine whether the new CO band will be observed, we also do not believe that the charge of the surface oxide affects the presence of the additional band. For instance, KOH is strongly basic, and the excess (alkali) oxide could be donating electron density to adjacent platinum atoms affecting the number of CO bands. A comparison of the amount of potassium, in excess of the structural aluminum, with the infrared spectra shows no correlation; refer to Table 1. For example Pt/K^+ FAU(Y), Pt/K^+ β, Pt/K^+ MOR, and Pt/K^+ MAZ all have more excess potassium than Pt/K^+ LTL, yet the former display only one linear- and one bridge-bonded CO absorption.

According to the second hypothesis, the additional band is thought to arise from an electrostatic interaction, for example an ion–dipole attraction, of the oxygen atom of the linearly adsorbed CO with the alkali cation (*14, 45–49*). The additional attraction strengthens the bond and lowers the CO stretching frequency. We believe that this proposal is consistent with our results. In some zeolites, it appears that the position of the cation and platinum is such that only one environment exists for linear bonded CO, whereas in other zeolites, such as LTL, MFI, and MTW, two environments exist. For example, one CO may be oriented through the pore window while a second CO may be oriented toward an alkali cation near the wall. If the presence of the additional band is associated with the two environments, these two environments readily exist in potassium-exchanged LTL, MFI, MTW, and K^+ SiO_2; hence, the spectra exhibit the additional infrared absorbance band. On the other hand, other zeolites may not have these two environments. For Pt/Na^+ FAU(Y), the 1990 cm^{-1} infrared band is observed only after heating to 573 K for 16 h in CO (*33*). It is possible that at elevated temperatures in the presence of CO the platinum or alkali may migrate and may create the same two environments that readily exist in LTL, MFI, MTW, and K^+ SiO_2 without high-temperature treatment.

While three CO infrared bands are observed on some nonacidic platinum zeolite/catalysts, for example, Pt/K^+ LTL, only two infrared bands were observed for Pt/H^+ LTL. If the additional band arises from the interaction of the oxygen of CO and the cation, in the absence of cation no band should be observed (Figs. 3–5). Indeed, that is what is observed. In Pt/La^{3+} LTL, potassium ions were exchanged by oxophilic lanthanum (3 +) ions. One might expect that if the CO–cation interaction were purely electrostatic in origin, the three bands should be observed for Pt/La^{3+} LTL. The occurrence of only two absorption bands implies that in addition to the proper orientation of the adsorbed CO and the cation, the surface must be nonacidic.

Catalytic performance and infrared spectra. Comparison of the catalytic results for *n*-hexane aromatization with the infrared spectra shows little correspondence of activity or selectivity with the presence of the new infrared band. For example, in Table 5, Pt/K^+ LTL, with three infrared bands, is the most selective catalyst for one-six ring closure. The next most selective catalyst, as determined by the one-six/one-five ring closure ratio, is Pt/K^+ MAZ, which exhibits only two infrared bands. On the other hand, Pt/K^+ MFI, Pt/K^+ MTW, and Pt/K^+ SiO_2, catalysts with three infrared bands, have a lower one-six ring closure selectivity than Pt/K^+ LTL. For the former, the selectivity ratio for ring closure is also very similar to catalysts exhibiting only two infrared bands; for example, compare Pt/K^+ β or Pt/K^+ GME.

A similar conclusion can be drawn by comparison of the catalytic activity in Table 6 with the infrared spectra. Although Pt/K^+ LTL has the highest specific activity for formation of benzene, Pt/K^+ β and Pt/K^+ MAZ are each very active. By contrast, Pt/K^+ MFI, Pt/K^+ MTW, and Pt/K^+ SiO_2 have low activity. In general, we find no relationship between the number (or frequency) of infrared bands and the catalytic performance for hexane aromatization. However, the presence of the additional band has been shown to be dependent on the temperature treatment (*33*), and the catalytic environment at reaction temperature may differ from that at room temperature, where the infrared spectra were collected.

CONCLUSION

The infrared spectra of adsorbed CO for the nine platinum, potassium-exchanged zeolites all show a strong absorbance around 2070 ± 20 cm^{-1} due to linear-adsorbed CO and a weaker absorbance around 1850 ± 20 cm^{-1} due to bridge-bonded CO. On potassium-exchanged LTL, MFI, MTW, and alkalized SiO_2, there is an additional infrared absorbance near 1970 cm^{-1}. Both adsorption and desorption of CO indicate that the additional band behaves similarly to the linear-bonded CO band. At the same time, surface coverage experiments indicate that the additional band and linear-bonded CO band are independent bands and do not, therefore, result from a *gem*-dicarbonyl. Although three infrared bands are present on Pt/K^+ LTL, Pt/K^+ MFI, Pt/K^+ MTW, and Pt/K^+ SiO_2, the new (linear) CO band is absent in (alkali-free) silica, La^{3+} LTL, H^+ LTL, and H^+ MFI, i.e., neutral and acidic supports. The occurrence of three infrared bands is not attributed to a bimodal distribution of platinum inside the zeolite pores, nor to the negatively charged surface oxide ions in aluminum-rich zeolites. In addition, the infrared spectra of Pd/K^+ LTL and Pd/Ba^{2+} LTL show that the additional CO band is not unique to platinum. In the palladium LTL catalysts, the size and shape of the new infrared band were similar to the linear CO band at 2075 cm^{-1}, consistent with the assignment of the new band to linearly bonded CO.

It is speculated that the structure of the support influences the location of the potassium ions relative to platinum and linearly adsorbed CO. In some basic catalysts, two environments are created: one giving rise to the typical linear-bonded CO and a second giving rise to the additional band due to the CO–alkali interaction. The electrostatic attraction of the alkali with the oxygen atom increases the CO adsorption strength, decreasing the infrared stretching frequency.

The catalytic activity or selectivity for aromatization of *n*-hexane did not correspond to any feature of the infrared spectra. Neither the occurrence of the additional band nor the frequency of the additional band could be associated with catalytic performance. Although it has been shown that good catalysts for hexane aromatization require nonacidic supports, and for a given zeolite, the catalytic selectivity increases with increasing basicity of the support, it also appears that basicity alone cannot predict which support will yield an active and selective catalyst. Of the zeolites examined, the most selective catalysts for one-six ring closure, i.e., Pt/K^+ LTL and Pt/K^+ MAZ, have similar geometries with one-dimensional pores and large internal cavities.

ACKNOWLEDGMENTS

The authors acknowledge J. L. Yedinak, J. B. Hall, C. Choi-Feng, B. Meyers, and P. D. Hopkins.

REFERENCES

1. Little, L. H., "Infrared Spectra of Adsorbed Species." Academic Press, New York, 1966.
2. Hair, M. L., "Infrared Spectroscopy in Surface Chemistry." Dekker, New York, 1967.
3. Eischens, R. D., and Pliskin, W. A., *in* "Advances in Catalysis" (D. D. Eley, W. G. Frankenburg, and V. I. Komarewsky, Eds.), Vol. 10, p. 1. Academic Press, New York, 1958.
4. Eischens, R. D., Francis, S. A., and Pliskin, W. A., *J. Phys. Chem.* **60,** 194 (1956).
5. Peri, J. B., *J. Catal.* **52,** 144 (1978).
6. Rothchild, W. G., and Yoa, H. C., *J. Phys. Chem.* **74,** 4186 (1981).
7. Stoop, F., Toolenaar, J. C. M., and Ponec, V., *J. Catal.* **73,** 50 (1982).
8. Primet, M., *J. Catal.* **88,** 273 (1984).
9. Haaland, D. M., *Surf. Sci.* **185,** 1 (1987).
10. Barth, R., and Ramachandran, A., *J. Catal.* **125,** 467 (1990).
11. Ford, R. R., *in* "Advances in Catalysis" (D. D. Eley, H. Pines, and P. B. Weisz, Eds.), Vol. 21, p. 51. Academic Press, New York, 1970.
12. Bartok, M., Sarkany, J, and Sitkei, A., *J. Catal.* **72,** 236 (1981).
13. Sarkany, J., and Bartok, M., *J. Catal.* **92,** 388 (1985).
14. Boujana, S., Demri, D., Cressely, J., Kiennemann, A., and Hindermann, J. P., *Catal. Lett.* **7,** 359 (1990).
15. Pitchon, V., Primet, M., and Praliaud, H., *Appl. Catal.* **62,** 317 (1990).
16. Hayden, B. E., Kretzschmar, K., and Bradshaw, A. M., *Surf. Sci.* **149,** 394 (1985).
17. Hopster, H., and Ibach, H., *Surf. Sci.* **77,** 109 (1978).
18. Garland, C. W., Lord, R. C., and Troiano, P. F., *J. Phys. Chem.* **69,** 1188 (1965).
19. Garland, C. W., Lord, R. C., and Troiano, P. F., *J. Phys. Chem.* **69,** 1195 (1965).
20. Blyholder, G., and Sheets, R. J., *J. Phys. Chem.* **74,** 4335 (1980).
21. Shigeishi, R. A., and King, D. A., *Surf. Sci.* **58,** 379 (1976).
22. Crossley, A., and King, D. A., *Surf. Sci.* **68,** 528 (1977).
23. Gallezot, P., *Catal. Rev. Sci. Eng.* **20,** 121 (1979).
24. Primet, M., de Menorval, L.-C., and Fraissard, J., *J. Chem. Soc. Faraday Trans. I* **81,** 2867 (1985).
25. Figueras, F., Gomez, R., and Primet, M., "Molecular Sieves," Adv. Chem. Ser. (W. M. Meier and J. B. Uytterhoeven, Eds.), Vol. 121, p. 480. American Chemical Society, Washington D.C. 1973.
26. Naccache, C., Primet, M., and Mathier, M. V., "Molecular Sieves," Adv. Chem. Ser. (W. M. Meier and J. B. Uytterhoeven, Eds.), Vol. 121, p. 266. American Chemical Society, Washington D.C. 1973.
27. Gallezot, P., Datka, J., Massardier, J., Primet, M., and Imelik, B., *in* "Proceedings, 6th International Congress on Catalysis, London, 1976 (G. C. Bond, P. B. Wells, and F. C. Tompkins, Eds.), Vol. 2, p. 696. The Chemical Society, London, 1977.
28. Chukin, G. D., Landau, M. V., Kruglikov, V., Agievskii, D. A., Smirnov, B. V., Belozerkov, A. L., Asrieva, V. D., Goncharova, N. V., Radchenko, E. D., Konovalcherov, O. D., and Agafonoy, A. V., *in* "Proceedings, 6th International Congress on Catalysis, London, 1976" (G. C. Bond, P. B. Wells, and F. C. Tompkins, Eds.), Vol. 1, p. 668. The Chemical Society, London, 1977.
29. De Mallman, A., and Barthomeuf, D., *Catal. Lett.* **5,** 293 (1990).
30. Besoukhanova, C., Breysse, M., Bernard, J. R., and Barthomeuf, D., *in* "Proceedings, 7th International Congress on Catalysis, Tokyo, 1980" (T.

Seiyama and K. Tanabe, Eds.), p. 1410. Elsevier, Amsterdam, 1981.

31. Besoukhanova, C., Guidot, J., Barthomeuf, D., Breysse, M., and Bernard, J. R., *J. Chem. Soc. Faraday Trans. 1* **77**, 1595 (1981).

32. Besoukhanova, C., Breysse, M., Bernard, J. R., and Barthomeuf, D., *in* "Studies in Surface Science and Catalysis," Vol. 6, "Catalyst Deactivation," p. 201. Elsevier, Amsterdam, 1980.

33. De Mallmann, A., and Barthomeuf, D., *in* "Studies in Surface Science and Catalysis" Vol. 46, "Zeolites as Catalysts, Sorbents, and Detergent Builders-Applications and Innovation," p. 1410. Elsevier, Amsterdam, 1989.

34. Argaur, R. J., and Landolt, G. R., (Mobil) U.S. Patent 3,702,886 (1972).

35. Jacobs, P. A., and Martens, J. A., *in* "Studies in Surface Science and Catalysis," Vol. 33, "Synthesis of High-Silica Aluminosilicate Zeolites," p. 13. Elsevier, Amsterdam, 1987.

36. Breck, D. W., (Union Carbide) U.S. Patent 3,054,657 (1962).

37. Breck, D. W., "Zeolite Molecular Sieves, Structure, Chemistry and Use." p. 306.

38. Wadlinger, R. L., Kerr, G. T., and Rosinski, E. T., (Mobil) U.S. Patent 3,308,069 (1967).

39. Vaarkamp, M., Grondelle, J. V., Miller, J. T., Sajkowski, D. J., Modica, F. S., Lane, G. S., Gates, B. C., and Koningsberger, D. C., *Catal. Lett.* **6**, 369 (1990).

40. Lane, G. S., Modica, F. S., and Miller, J. T., *J. Catal.* **129**, 145 (1991).

41. Yang, A. C., and Garland, C. W., *J. Phys. Chem.* **61**, 1504 (1957).

42. Tamm, P. W., Mohr, D. H., and Wilson, C. R., *in* "Studies in Surface Science and Catalysis," Vol. 38, "Catalysis 1987: Proceedings, 10th North American Meeting of the Catalysis Society," p. 335. Elsevier, Amsterdam, 1988.

43. Vaarkamp, M., Grondelle, J., van Santen, R. A., Koningsberger, D. C., Miller, J. T., Meyers, B. L., Lane, G. S., and Modica, F. S., *in* "Proceedings, 9th International Zeolite Conference, Montreal, 1992," in press.

44. Vaarkamp, M., Grondelle, J., Koningsberger, D. C., Miller, J. T., Modica, F. S., and Lane, G. S., *in* "Proceedings, 10th International Congress on Catalysis, Budapest, 1992," (L. Guczi, Ed.). Institute of Isotopes of the Hungarian Academy of Science, Budapest, 1992.

45. Praliaud, H., Primet, M., and Martin, G. A., *Bull. Soc. Chim.* **5**, 719 (1986).

46. Praliaud, H., Primet, M., and Martin, G. A., *Appl. Surf. Sci.* **17**, 107 (1983).

47. Angevaare, P. A. J. M., Hendrickx, H. A. C. M., and Ponec, V. J., *J. Catal.* **110**, 11 (1988).

48. Angevaare, P. A. J. M., Hendrickx, H. A. C. M., and Ponec, V. J., *J. Catal.* **110**, 18 (1988).

49. Zecchina, A., Bordiga, S., Platero, E. E., and Arean, C. O., *J. Catal.* **125**, 568 (1990).